17

Modelling Evapotranspiration and the Surface Energy Budget in Alpine Catchments

Giacomo Bertoldi[1], Riccardo Rigon[2] and Ulrike Tappeiner[1,3]
[1] *Institute for Alpine Environment, EURAC Research, Bolzano.*
[2] *University of Trento.*
[3] *Institute of Ecology, University of Innsbruck.*
[1,2] *Italy*
[3] *Austria.*

1. Introduction

Accurate modelling of evapotranspiration (ET) is required to predict the effects of climate and land use changes on water resources, agriculture and ecosystems. Significant progress has been made in estimating ET at the global and regional scale. However, further efforts are needed to improve spatial accuracy and modeling capabilities in alpine regions (Brooks & Vivoni, 2008b). This chapter will point out the components of the energy budget needed to model ET, to discuss the fundamental equations and to provide an extended review of the parametrizations available in the hydrological and land surface models literature. The second part of the chapter will explore the complexity of the energy budget with special reference to mountain environments.

2. The energy budget components

Evapotranspiration is controlled by the surface water and energy budget. In this section the single components of the energy budget will be discussed: radiation, soil heat flux, sensible and latent heat fluxes.
The surface energy budget inside a control volume can be written as:

$$\Delta t \left(R_n - H - LE - G\right) = \Delta E \tag{1}$$

where the energy fluxes concerning the soil-atmosphere interface in the time interval Δt are:

- R_n net radiative flux;
- H sensible heat flux;
- LE latent heat flux;
- G heat flux in the soil;
- ΔE internal energy variation in the control volume;

The control volume is assumed with a thickness of some meters, so as to include the soil layer close to the surface and the first meters of the atmosphere, including the possible vegetation cover.

Besides the surface energy budget also the mass budget must be considered in order to quantify ET, namely the water conservation inside the control volume.

$$\frac{\Delta S}{\Delta t} = P - ET - R - R_G - R_S \tag{2}$$

where ΔS is the storing of the various supplies (underground and surface storage, soil moisture, vegetation interception, storing in channels); P is precipitation; $ET = \lambda LE$ is evapotranspiration; λ is the latent heat of vaporization; R is the surface runoff; R_G is the runoff towards the deep water table; R_S is the sub-surface runoff.
In the next sections it will be explained how the different components of the energy budget are usually described in hydrological and Land Surface Models (LSMs): radiation, sensible and latent heat flux, soil heat flux.

2.1 Radiation

The radiation is usually divided in short-wave components - indicated here as SW (including visible light, part of the ultraviolet radiation and the close infrared) and long-wave components - indicated here as LW (infrared radiation), with wavelength λ ranging respectively from 0.1 to 3 μm (98% of extraterrestrial radiation) and from 3 to 100 μm (2% of extraterrestrial radiation). In photosynthetic processes the short-wave radiation is further divided in photosynthetically active radiation ($0.4 < \lambda < 0.7 \mu m$) and near infrared (Bonan, 1996).
Moreover, there is a further distinction between diffuse radiation D (coming by diffusion in the atmosphere from any direction) and direct radiation P (coming only from the sun), and also between radiation from the sky downwards ("$down$" $\downarrow$) and radiation from the soil upwards ("up" $\uparrow$).
The net radiation at the soil level can be factorized as follows:

$$\begin{aligned} R_n = sw \cdot (R\downarrow_{SW\ P} + R\downarrow_{LW\ P}) + V \cdot (R\downarrow_{SW\ D} + R\downarrow_{LW\ D}) - \\ R\uparrow_{SW} - R\uparrow_{LW\ R} - R\uparrow_{LW} + R\downarrow_{SW\ O} + R\downarrow_{LW\ O} \end{aligned} \tag{3}$$

with:

$R\downarrow_{SW\ P}$	short-wave direct radiation;
$R\downarrow_{LW\ P}$	long-wave direct radiation;
$R\downarrow_{SW\ D}$	short-wave diffuse radiation;
$R\downarrow_{LW\ D}$	long-wave diffuse radiation;
$R\uparrow_{SW}$	short-wave reflected radiation;
$R\uparrow_{LW\ R}$	long-wave reflected radiation;
$R\uparrow_{LW}$	radiation emitted by surface;
$R\downarrow_{SW\ O} + R\downarrow_{LW\ O}$	reflected radiation emitted by the surrounding surfaces;

The effects of topography on the diffused radiation can be expressed through the sky view factor V, indicating the sky fraction visible in one point.
In the presence of reliefs only part of the horizon is visible and this has consequences on the radiative exchanges.
V is defined as:

$$V = \omega / 2\pi \tag{4}$$

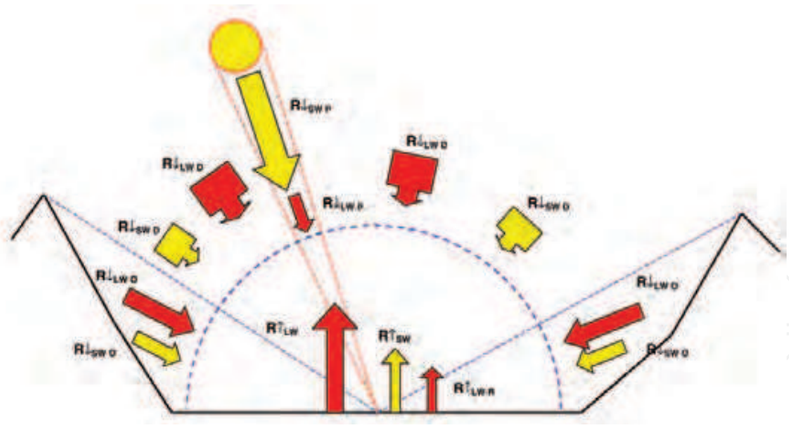

Fig. 1. Scheme of the solar radiation components.

where ω is the solid angle seen from the point considered.
The presence of shadows due to surrounding mountains can be expressed through a factor sw, a function of topography and sun position, defined as:

$$sw = \begin{cases} 1 \text{ if the point is in the sun} \\ 0 \text{ if the point is in the shadow} \end{cases} \tag{5}$$

All direct radiation terms have to be multiplied by this factor.
In the next paragraphs we analyze in detail the parametrization of the single terms composing the radiation flux.

2.1.1 Direct radiation $R\downarrow_{SW\ P}$ and $R\downarrow_{LW\ P}$

The direct long-wave radiation $R\downarrow_{LW\ P}$ is emitted directly by the sun and therefore it is negligible at the soil level (differently from the long-wave diffuse radiation).
Usually the short-wave radiation $R\downarrow_{SW\ P}$ is assumed as an input variable, measured or calculated by an atmospheric model. The direct radiation can be written as the product of the extraterrestrial radiation R_{Extr} by an attenuation factor varying in time and space.

$$R\downarrow_{SW\ P} = F_{att} R_{Extr} \tag{6}$$

The extraterrestrial radiation can be easily calculated on the basis of geometric formulas (Iqbal, 1983). The atmospheric attenuation is due to Rayleigh diffusion, to the absorption on behalf of ozone and water vapor, to the extinction (both diffusion and absorption) due to atmospheric dust and shielding caused by the possible cloud cover. Moreover the absorption entity depends on the ray path length through the atmosphere, a function of the incidence angle and of the measurement point elevation. The effect of the latter can be very important in a mountain environment, where it is necessary to consider the shading effects.
Part of the dispersed radiation is then returned as short-wave diffuse radiation ($R\downarrow_{SW\ D}$) and part of the energy absorbed by atmosphere is then re-emitted as long-wave diffuse radiation ($R\downarrow_{LW\ D}$).
From a practical point of view, according to the application type and depending on the measured data possessed, the attenuation coefficient can be calculated with different degrees of complexity. The radiation transfer through the atmosphere is a well studied phenomenon

and there exist many models providing the soil incident radiation spectrum in a detailed way, considering the various attenuation effects separately (Kondratyev, 1969).

2.1.2 Diffuse downward short-wave radiation $R\downarrow_{SW\ D}$

This term is a function of the atmospheric radiation due to Rayleigh dispersion and to the aereosols dispersion, as well as to the presence of cloud cover. The $R\downarrow_{SW\ D}$ actually is not isotropic and it depends on the sun position above the horizon. For its parametrization, see, for example, Paltrige & Platt (1976).

2.1.3 Diffuse downward long-wave radiation $R\downarrow_{LW\ D}$

Often this term in not provided by standard meteorological measurements, and many LSMs provide expressions to calculate it. This term indicates the long-wave radiation emitted by atmosphere towards the earth. It can be calculated starting from the knowledge of the distribution of temperature, humidity and carbon dioxide of the air column above. If this information is not available, various formulas, based only on ground measurements, can be found in literature with expressions as follows:

$$R\downarrow_{LW\ D} = \epsilon_a \sigma T_a^4 \tag{7}$$

with:

T_a air temperature [K];
ϵ_a atmosphere emissivity $f(e_a, T_a,$ cloud cover$)$;
e_a vapor pressure [mb];

Usually for ϵ_a empirical formulas have been used, but it is also possible to provide a derivation based on physical topics like in Prata (1996). The cloud cover effect on this term is significant and not easy to consider in a simple way. Cloud cover data can be provided during the day by ground or satellite observations but, especially on night, is difficult to collect.

2.1.4 Reflected short-wave radiation $R\uparrow_{SW}$

This term indicates the short-wave energy reflection.

$$R\uparrow_{SW} = a(R\downarrow_{SW\ P} + R\downarrow_{SW\ D}) \tag{8}$$

where a is the albedo.
The albedo depends strongly on the wave length, but generally a mean value is used for the whole visible spectrum. Besides its dependance on the surface type, it is important to consider its dependence on soil water content, vegetation state and surface roughness. The albedo depends moreover on the sun rays inclination, in particular for smooth surfaces: for small angles it increases. There is very rich literature about albedo description, it being a key parameter in the radiative exchange models, see for example Kondratyev (1969). Albedo is often divided in visible, near infrared, direct and diffuse albedo, as in Bonan (1996).

2.1.5 Long-wave radiation emitted by the surface $R\uparrow_{LW}$

This term indicates the long-wave radiation emitted by the earth surface, considered as a grey body with emissivity ε_s (values from 0.95 to 0.98). The surface temperature $T_s\ [K]$ is unknown

and must be calculated by a LSM. $\sigma = 5.6704 \cdot 10^{-8}\ W/(m^2K^4)$ is Stefan-Boltzman constant.

$$R \uparrow_{LW} = \varepsilon_s \sigma T_s^4 \tag{9}$$

2.1.6 Reflected long-wave radiation $R \uparrow_{LW\ R}$

This term is small and can be subtracted by the incoming long-wave radiation, assuming surface emissivity ε_s equal to surface absorptivity:

$$R \downarrow_{LW\ D} = \varepsilon_s \cdot \epsilon_a \sigma T_a^4 \tag{10}$$

2.1.7 Radiation emitted and reflected by surrounding surfaces $R \downarrow_{SW\ O} + R \downarrow_{LW\ O}$

It indicates the radiation reflected ($R \uparrow_{SW} + R \uparrow_{LW\ R}$) and emitted ($R \uparrow_{LW}$) by the surfaces adjacent to the point considered. This term is important at small scale, in the presence of artificial obstructions or in the case of a very uneven orography. To calculate it with precision it is necessary to consider reciprocal orientation, illumination, emissivity and the albedo of every element, through a recurring procedure (Helbig et al., 2009). A simple solution is proposed for example in Bertoldi et al. (2005).
If the intervisible surfaces are hypothesized to be in radiative equilibrium, i.e. they absorb as much as they emit, these terms can be quantified in a simplified way:

$$\begin{aligned} R \downarrow_{SW\ O} &= (1 - V) R \uparrow_{SW} \\ R \downarrow_{LW\ O} &= (1 - V)(R \uparrow_{LW} + R \uparrow_{LW\ R}) \end{aligned} \tag{11}$$

2.1.8 Net radiation

Inserting expressions (7) and (9) in the (3), the net radiation is:

$$R_n = [sw \cdot R \downarrow_{SW\ P} + V \cdot R \downarrow_{SW\ D}](1 - V \cdot a) + V \cdot \varepsilon_s \cdot \varepsilon_a \cdot \sigma \cdot T_a^4 - V \cdot \varepsilon_s \cdot \sigma \cdot T_s^4 \tag{12}$$

with $\varepsilon_a = f(e_a, T_a,$ cloud cover$)$ as for example in Brutsaert (1975).
Equation (12) is not invariant with respect to the spatial scale of integration: indeed it contains non-linear terms in T_a, T_s, e_a, consequently the same results are not obtained if the local values of these quantities are substituted by the mean values of a certain surface. Therefore, the shift from a treatment valid at local level to a distributed model valid over a certain spatial scale must be done with a certain caution.

2.1.9 Radiation adsorption and backscattering by vegetation

Expression (12) needs to be modified to take into account the radiation adsorption and backscattering by vegetation, as shown in Figure 2. This effect is very important to obtain a correct soil surface skin temperature (Deardorff, 1978). From Best (1998) it is possible to derive the following relationship:

$$\begin{aligned} R_n = [sw \cdot R \downarrow_{SW\ P} + V \cdot R \downarrow_{SW\ D}](1 - V \cdot a) * (f_{trasm} + a_v) \\ + (1 - \varepsilon_v) \cdot V \cdot \varepsilon_s \cdot \varepsilon_a \cdot \sigma \cdot T_a^4 + \varepsilon_v \cdot \varepsilon_s \cdot \sigma \cdot T_v^4 \end{aligned} \tag{13}$$

where T_v is vegetation temperature, ε_v vegetation emissivity (supposed equal to absorption), a_v vegetation albedo (downward albedo supposed equal to upward albedo) and f_{trasm}

vegetation transmissivity, depending on plant type, leaf area index and photosynthetic activity.
Models oriented versus ecological applications have a very detailed parametrization of this term (Dickinson et al., 1986). Bonan (1996) uses a two-layers canopy model. Law et al. (1999) explicit the relationship between leaf area distribution and radiative transfer. A first energy budget is made at the canopy cover layer, and the energy fluxes are solved to find the canopy temperature, then a second energy budget is made at the soil surface. Usually a fraction of the grid cell is supposed covered by canopy and another fraction by bare ground.

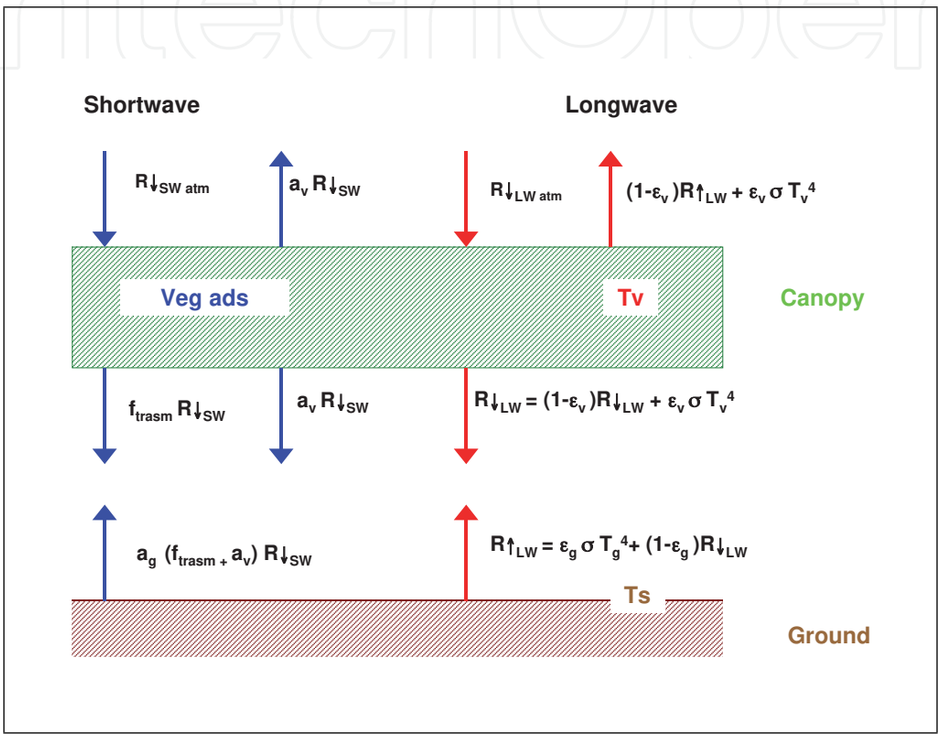

Fig. 2. Schematic diagram of short-wave radiation (left) and long-wave radiation (right) absorbed, transmitted and reflected by vegetation and ground , as in equation 13 (from Bonan (1996), modified).

2.2 Soil heat flux

The soil heat flux G at a certain depth z depends on the temperature gradient as follows:

$$G = -\lambda_s \frac{\partial T_s}{\partial z} \tag{14}$$

where λ_s is the soil thermal conductivity ($\lambda_s = \rho_s c_s \kappa_s$ with ρ_s density, c_s specific heat and κ_s soil thermal diffusivity) depending strongly on the soil saturation degree. The heat transfer inside the soil can be described in first approximation with Fourier conduction law:

$$\frac{\partial T_s}{\partial t} = \kappa_s \frac{\partial^2 T_s}{\partial z^2} \tag{15}$$

Equation (14) neglects the heat associated to the vapor transportation due to a vertical gradient of the soil humidity content as well as the horizontal heat conduction in the soil. The vapor transportation can be important in the case of dry climates (Saravanapavan & Salvucci, 2000). The soil heat flux can be calculated with different degrees of complexity. The most simple assumption (common in weather forecast models) is to calculate G as a fraction of net radiation (Stull (1988) suggests $G = 0.1R_n$). Another simple approach is to use the analytical solution for a sinusoidal temperature wave. A compromise between precision and computational work is the force restore method (Deardorff, 1978; Montaldo & Albertson, 2001), still used in many hydrological models (Mengelkamp et al., 1999). The main advantage is that only two soil layers have to be defined: a surface thin layer, and a layer getting down to a depth where the daily flux is almost zero. The method uses some results of the analytical solution for a sinusoidal forcing and therefore, in the case of days with irregular temperature trend, it provides less precise results.
The most general solution is the finite difference integration of the soil heat equation in a multilayered soil model (Daamen & Simmonds, 1997). However, this method is computationally demanding and it requires short time steps to assure numerical stability, given the non-linearity and stationarity of the surface energy budget, which is the upper boundary condition of the equation.

2.2.1 Snowmelt and freezing soil

In mountain environments snow-melt and freezing soil should be solved at the same time as soil heat flux. A simple snow melt model is presented in Zanotti et al. (2004), which has a lumped approach, using as state variable the internal energy of the snow-pack and of the first layer of soil. Other models consider a multi-layer parametrization of the snowpack (e.g. Bartelt & Lehning, 2002; Endrizzi et al., 2006). Snow interception by canopy is described for example in Bonan (1996). A state of the art freezing soil modeling approach can be found in Dall'Amico (2010) and Dall'Amico et al. (2011).

2.3 Turbulent fluxes

A modeling of the ground heat and vapor fluxes cannot leave out of consideration the schematization of the atmospheric boundary layer (ABL), meant as the lower part of atmosphere where the earth surface properties influence directly the characteristics of the motion, which is turbulent. For a review see Brutsaert (1982); Garratt (1992); Stull (1988).
A flux of a passive tracer x in a turbulent field (as for example heat and vapor close to the ground), averaged on a suitable time interval, is composed of three terms: the first indicates the transportation due to the mean motion v, the second the turbulent transportation $\overline{x' \mathbf{v}'}$, the third the molecular diffusion k.

$$\overline{\mathbf{F}} = \overline{x}\,\overline{\mathbf{v}} + \overline{x'\,\mathbf{v}'} - k\nabla x \tag{16}$$

The fluxes parametrization used in LSMs usually only considers as significant the turbulent term only. The molecular flux is not negligible only in the few centimeters close the surface, and the horizontal homogeneity hypothesis makes negligible the convective term.

2.3.1 The conservation equations

The first approximation done by all hydrological and LSMs in dealing with turbulent fluxes is considering the Atmospheric Boundary Layer (ABL) as subject to a stationary, uniform motion, parallel to a plane surface.
This assumption can become limitative if the grid size becomes comparable to the vertical heterogeneity scale (for example for a grid of 10 m and a canopy height of 10 m). In this situation horizontal turbulent fluxes become relevant. A possible approach is the Large Eddy Simulation (Albertson et al., 2001).
If previous assumptions are made, then the conservation equations assume the form:

- Specific humidity conservation, failing moisture sources and phase transitions:

$$k_v \frac{\partial^2 \overline{q}}{\partial z^2} - \frac{\partial}{\partial z}(\overline{w'q'}) = 0 \tag{17}$$

  where:
  k_v is the vapor molecular diffusion coefficient $[m^2/s]$
  $q = \frac{m_v}{m_v + m_d}$ is the specific humidity [vapor mass out of humid air mass].

- Energy conservation:

$$k_h \frac{\partial^2 \overline{\theta}}{\partial z^2} - \frac{\partial}{\partial z}(\overline{w'\theta'}) - \frac{1}{\rho c_p}\frac{\partial H_R}{\partial z} = 0 \tag{18}$$

  where:
  k_h is the thermal diffusivity $[m^2/s]$
  H_R is the radiative flux $[W/m^2]$
  θ is the potential temperature [K]
  ρ is the air density $[kg/m^3]$
  w is the vertical velocity $[m/s]$.

- The horizontal mean motion equations are obtained from the momentum conservation by simplifying Reynolds equations (Stull, 1988; Brutsaert, 1982 cap.3):

$$-\frac{1}{\rho}\frac{\partial \overline{p}}{\partial x} + 2\omega \, sin\, \phi \, \overline{v} + \nu \frac{\partial^2 \overline{u}}{\partial z^2} - \frac{\partial}{\partial z}(\overline{w'u'}) = 0 \tag{19}$$

$$-\frac{1}{\rho}\frac{\partial \overline{p}}{\partial y} - 2\omega \, sin\, \phi \, \overline{u} + \nu \frac{\partial^2 \overline{v}}{\partial z^2} - \frac{\partial}{\partial z}(\overline{w'v'}) = 0 \tag{20}$$

  where:
  ν is the kinematic viscosity $[m^2/s]$
  ω is the earth angular rotation velocity [rad/s]
  ϕ is the latitude [rad] .

  The vertical motion equation can be reduced to the hydrostatic equation:

$$\frac{\partial p}{\partial z} = -\rho g. \tag{21}$$

In a turbulent motion the molecular transportation terms of the momentum, heat and vapor quantity, respectively ν, k_h and k_v, are several orders of magnitude smaller than Reynolds fluxes and can be neglected.

2.3.2 Wind, heat and vapor profile at the surface

Inside the ABL we can consider, with a good approximation, that the decrease in the fluxes intensity is linear with elevation. This means that in the first meters of the air column the fluxes and the friction velocity u^* can be considered constant. Considering the momentum flux constant with elevation implies that also the wind direction does not change with elevation (in the layer closest to the soil, where the geostrofic forcing is negligible). In this way the alignment with the mean motion allows the use of only one component for the velocity vector, and the problem of mean quantities on uniform terrain becomes essentially one-dimensional, as these become functions of the only elevation z.

In the first centimeters of air the energy transportation is dominated by the molecular diffusion. Close to the soil there can be very strong temperature gradients, for example during a hot summer day. Soil can warm up much more quickly than air. The air temperature diminishes very rapidly through a very thin layer called *micro layer*, where the molecular processes are dominant. The strong ground gradients support the molecular conduction, while the gradients in the remaining part of the surface layer drive the turbulent diffusion. In the remaining part of the surface layer the potential temperature diminishes slowly with elevation.

The effective turbulent flux in the interface sublayer is the sum of molecular and turbulent fluxes. At the surface, where there is no perceptible turbulent flux, the effective flux is equal to the molecular one, and above the first cm the molecular contribution is neglegible. According to Stull (1988), the turbulent flux measured at a standard height of 2 m provides a good approximation of the effective ground turbulent flux.

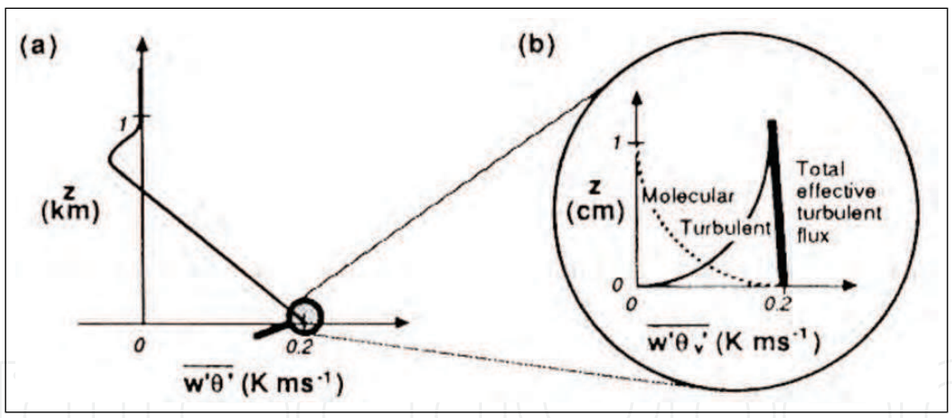

Fig. 3. (a) The effective turbulent flux in diurnal convective conditions can be different from zero on the surface. (b) The effective flux is the sum of the turbulent flux and the molecular flux (from Stull, 1988).

Applying the concept of effective turbulent flux, the molecular diffusion term can be neglected, while the hypothesis of uniform and stationary limit layer leads to neglect the convective terms due to the mean vertical motion and the horizontal flux. The vertical flux at the surface can then be reduced to the turbulent term only:

$$\overline{\mathbf{F_z}} = \overline{x' \, w'} \tag{22}$$

In the case of the water vapor, equation (17) shows that, if there is no condensation, the flux is:

$$ET = \lambda\rho\overline{w'q'} \tag{23}$$

where ET is the evaporation quantity at the surface, ρ the air density and λ is the latent heat of vaporization.
Similarly, as to sensible heat, equation (18) shows that the heat flux at the surface H is:

$$H = \rho c_p\overline{w'\theta'} \tag{24}$$

where c_p is the air specific heat at constant pressure.
The entity of the fluctuating terms $\overline{w'u'}$, $\overline{w'\theta'}$ and $\overline{w'q'}$ remains unknown if further hypotheses (called closing hypotheses) about the nature of the turbulent motion are not introduced. The closing model adopted by the LSMs is Bousinnesq model: it assumes that the fluctuating terms can be expressed as a function of the vertical gradients of the quantities considered (diffusive closure).

$$\tau_x = -\rho\overline{u'w'} = \rho K_M \partial\overline{u}/\partial z \tag{25}$$

$$H = -\rho c_p\overline{w'\theta'} = -\rho c_p K_H \partial\overline{\theta}/\partial z \tag{26}$$

$$ET = -\lambda\rho\overline{w'q'} = -\rho K_W \partial\overline{q}/\partial z \tag{27}$$

where K_M is the turbulent viscosity, K_H and K_W $[m^2/s]$ are turbulent diffusivity. Moreover a logarithmic velocity profile in atmospheric neutrality conditions is assumed:

$$\frac{k\,u}{u_{*0}} = \ln(\frac{z}{z_o}) \tag{28}$$

where k is the Von Karman constant, z_0 is the aerodynamic roughness, evaluated in first approximation as a function of the height of the obstacles as $z_0/h_c \simeq 0.1$ (for more precise estimates see Stull (1988) p.379; Brutsaert (1982) ch.5; Garratt (1992) p.87). In the case of compact obstacles (e.g. thick forests), the profile can be thought of as starting at a height d_0, and the height z can be substituted with a fictitious height $z - d_0$.

Surface type	z_0 [cm]
Large water surfaces	0.01-0.06
Grass, height 1 cm	0.1
Grass, height 10 cm	2.3
Grass, height 50 cm	5
Vegetation, height 1-2 m	20
Trees, height 10-15 m	40-70
Big towns	165

Table 1. Values of aerodynamic roughness length z_0 for various natural surfaces (from Brutsaert, 1982).

Also the other quantities θ and q have an analogous distribution. Using as scale quantities $\theta_{*0} = -\overline{w'\theta'}_0/u_{*0}$ e $q_{*0} = -\overline{w'q'}_0/u_{*0}$ and substituting them in the (25), the following

integration is obtained:

$$\frac{k(\theta - \theta_0)}{\theta_{*0}} = \ln(\frac{z}{z_T}) \tag{29}$$

$$\frac{k(q - q_0)}{q_{*0}} = \ln(\frac{z}{z_q}). \tag{30}$$

The boundary condition chosen is $\theta = \theta_0$ in $z = z_T$ and $q = q_0$ in $z = z_q$. The temperature θ_0 then is not the ground temperature, but that at the elevation z_T. The roughness height z_T is the height where temperature assumes the value necessary to extrapolate a logarithmic profile. Analogously, z_q is the elevation where the vapor concentration assumes the value necessary to extrapolate a logarithmic profile.
Indeed, close to the soil (interface sublayer) the logarithmic profile is not valid and then, to estimate z_T and z_q, it would be necessary to study in a detailed way the dynamics of the heat and mass transfer from the soil to the first meters of air.
If we consider a real surface instead of a single point, the detail requested to reconstruct accurately the air motion in the upper soil meters is impossible to obtain. Then there is a practical problem of difficult solution: on the one hand, the energy transfer mechanisms from the soil to the atmosphere operate on spatial scales of few meters and even of few cm, on the other hand models generally work with a spatial resolution ranging from tens of m (as in the case of our approach) to tens of km (in the case of mesoscale models). Models often apply to local scale the same parametrizations used for mesoscale. Therefore a careful validation test, even for established theories, is always important.
Observations and theory (Brutsaert, 1982, p.121) show that z_T and z_q generally have the same order of magnitude, while the ratio $\frac{z_T}{z_0}$ is roughly included between $\frac{1}{5} - \frac{1}{10}$.

2.3.3 The atmospheric stability

In conditions different from neutrality, when thermal stratification allows the development of buoyancies, Monin & Obukhov (1954) similarity theory is used in LSMs. The similarity theory wants to include the effects of thermal stratification in the description of turbulent transportation. The stability degree is expressed as a function of Monin-Obukhov length, defined as:

$$L_{MO} = -\frac{u_{0*}^3 \theta_0}{kg\overline{w'\theta'}} \tag{31}$$

where θ_0 is the potential temperature at the surface.
Expressions of the stability functions can be found in many texts of Physics of the Atmosphere, for example Katul & Parlange (1992); Parlange et al. (1995). The most known formulation is to be found in Businger et al. (1971). Yet stability is often expressed as a function of bulk Richardson number Ri_B between two reference heights, expresses as:

$$Ri_B = \frac{g\ z\ \Delta\theta}{\overline{\theta} u^2} \tag{32}$$

where $\Delta\theta$ is the potential temperature difference between two reference heights, and $\overline{\theta}$ is the mean potential temperature.

If $Ri_B > 0$ atmosphere is steady, if $Ri_B < 0$ atmosphere is unsteady. Differently from L_{MO}, Ri_B is also a function of the dimensionless variables z/z_0 e z/z_T. The use of Ri_B has the advantage that it does not require an iterative scheme.
Expressions of the stability functions as a function of Ri_B are provided by Louis (1979) and more recently by Kot & Song (1998). Many LSMs use empirical functions to modify the wind profile inside the canopy cover.
From the soil up to an elevation $h_d = f(z_0)$, limit of the interface sublayer, the logarithmic universal profile and Reynolds analogy are no more valid. For smooth surfaces the interface sublayer coincides with the viscous sublayer and the molecular transport becomes important. For rough surfaces the profile depends on the distribution of the elements present, in a way which is not easy to parametrize. Particular experimental relations can be used up to elevation h_d, to connect them up with the logarithmic profile (Garratt, 1992, p. 90 and Brutsaert, 1982, p. 88). These are expressions of non-easy practical application and they are still little tested.

2.3.4 Latent and sensible heat fluxes

As consequence of the theory explained in the previous paragraph, the turbulent latent and sensible fluxes H and LE can be expressed as:

$$H = \rho c_p \overline{w'\theta'} = \rho c_p C_H u(\theta_0 - \theta) \tag{33}$$

$$ET = \lambda \rho \overline{w'q'} = \lambda \rho C_E u(q_0 - q), \tag{34}$$

where $\theta_0 - \theta$ and $q_0 - q$ are the difference between surface and measurement height of potential temperature and specific humidity respectively. C_H and C_E are usually assumed to be equal and depending on the bulk Richardson number (or on Monin-Obukhov lenght):

$$C_H = C_{Hn} F_H(Ri_B), \tag{35}$$

where C_{Hn} is the heat bulk coefficient for neutral conditions:

$$C_{Hn} = C_{En} = \frac{k^2}{[\ln(z/z_0)][\ln(z_a/z_T)]} \tag{36}$$

derived on Eq. 29 and depending on the wind speed u, the measurement height z, the temperature (or moisture) measurement height z_a, the momentum roughness length z_0 and the heat roughness length z_T.
A common approach is the 'electrical resistance analogy' (Bonan, 1996), where the atmospheric resistance is expressed as:

$$r_{aH} = r_{aE} = (C_H\, u)^{-1} \tag{37}$$

3. Evapotranspiration processes

In order to convert latent heat flux in evapotranspiration the energy conservation must be solved at the same time as water mass budget. In fact, there must be a sufficient water quantity available for evaporation. Moreover, vegetation plays a key role.

3.1 Unsaturated soil evaporation

If the availability of water supply permits to reach the surface saturation level, then evaporation is potential $ET = EP$ and then we have air saturation at the surface $q(T_s) = q^*(T_s)$ (the superscript * stands here for saturation). If the soil is unsaturated, $q(T_s) \neq q^*(T_s)$ and different approaches are possible to quantify the water content at the surface, in dependance of the water budget scheme adopted.

1. A first possibility is to introduce then the concept of surface resistance r_g to consider the moisture reduction with respect to the saturation value. As it follows from equation (34):

$$ET = \lambda\rho C_E u(q_0 - q) = \lambda\rho\frac{1}{r_a}(q_0 - q) = \lambda\rho\frac{1}{r_a + r_g}(q_0^* - q) \tag{38}$$

2. As an alternative, we can define a soil-surface relative moisture

$$r_h = q_0/q_0^* \tag{39}$$

and then the expression for evaporation becomes:

$$ET = \lambda\rho\frac{1}{r_a}(r_h\, q_0^* - q) \tag{40}$$

An expression of r_h as a function of the potential ψ_s [m] (work required to extract water from the soil against the capillarity forces) and of the ratio of the soil water content η to the saturation water content η_s is given in Philip & Vries (1957):

$$r_h = exp(-(g/R_v T_s)\psi_s(\eta/\eta_s)^{-b}) \tag{41}$$

where $R_v = 461.53\ [J/(kg\ K)]$ is the gas constant for water vapor, T_s is the soil temperature, b an empirical constant. Tables of these parameters for different soil types can be found in Clapp & Hornberger (1978).

Another more simple expression frequently applied in models to link the value r_h with the soil water content η is provided by Noilhan & Planton (1989):

$$r_h = \begin{cases} 0.5(1 - \cos(\frac{\eta}{\eta_k}\pi)) & se\ \eta < \eta_k \\ 1 & if\ \eta \geq \eta_k \end{cases} \tag{42}$$

where η is the moisture content of a soil layer with thickness d_1, and η_k is a critical value depending on the saturation water content: $\eta_k \simeq 0.75\eta_s$.

3. A third possibility, very used in large-scale models, is that of expressing the potential/real evaporation ration through a simple coefficient:

$$ET = x\ EP = x\ \lambda\rho\frac{1}{r_a}(q_0^* - q) \tag{43}$$

The value of x can be connected to the soil water content η through the expression (Deardorff, 1978) (see Figure 4):

$$x = min(1, \frac{\eta}{\eta_k}) \tag{44}$$

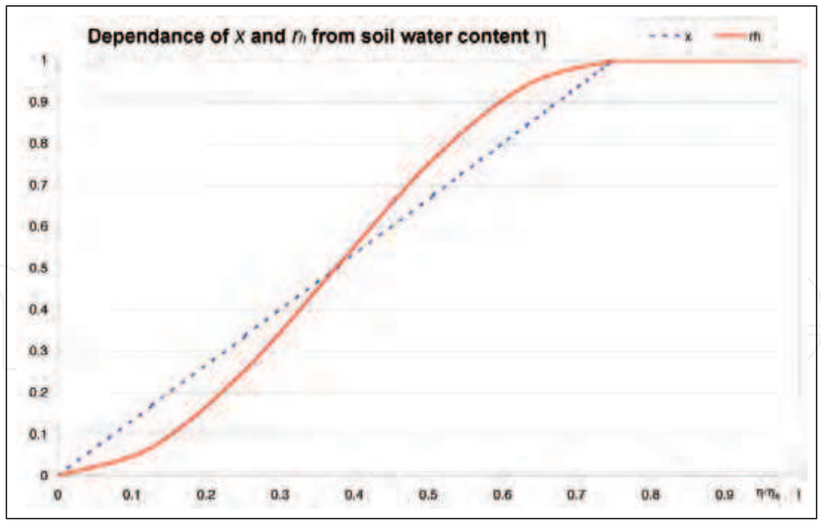

Fig. 4. Dependence of x and r_h on the soil water content η (Eq. 44-42)

3.2 Transpiration

Usually transpiration takes into account the canopy resistance r_c to add to the atmospheric resistance r_a:

$$ET = x\ EP = x\ \lambda\rho\frac{1}{r_a + r_c}(q_0^* - q) \tag{45}$$

The canopy resistance depends on plant type, leaf area index, solar radiation, vapor pressure deficit, temperature and water content in the root layer. There is a wide literature regarding such dependence, see for example Feddes et al. (1978); Wigmosta et al. (1994).

Canopy interception and evaporation from wet leaves are important processes modeled that should be modelled, according to Deardorff (1978). It is possible to distinguish two fundamental approaches: single-layer canopy models and multi-layer canopy models.

Single-layer canopy models (or "big leaf" models)

The vegetation resistance is entirely determined by stomal resistance and only one temperature value, representative of both vegetation and soil, is considered. Moreover a vegetation interception function can be defined so as to define when the foliage is wet or when the evaporation is controlled by stomal resistance.

Multi-layer canopy models

These are more complex models in which a soil temperature T_g, different from the foliage temperature T_f, is considered. Therefore, two pairs of equations of latent and sensible heat flux transfer, from the soil level to the foliage level, and from the latter to the free atmosphere, must be considered (Best, 1998). Moreover the equation for the net radiation calculation must consider the energy absorption and the radiation reflection by the vegetation layer.

Deardorff (1978) is the first author who presents a two-layer model with a linear interpolation between zones covered with vegetation and bare soil, to be inserted into atmosphere general circulation models. Over the last years many detailed models have been developed, above all with the purpose of evaluating the CO_2 fluxes between vegetation and atmosphere. Particularly complex is the case of scattered vegetation,

where evaporation is due to a combination of soil/vegetation effects, which cannot be schematized as a single layer (Scanlon & Albertson, 2003).

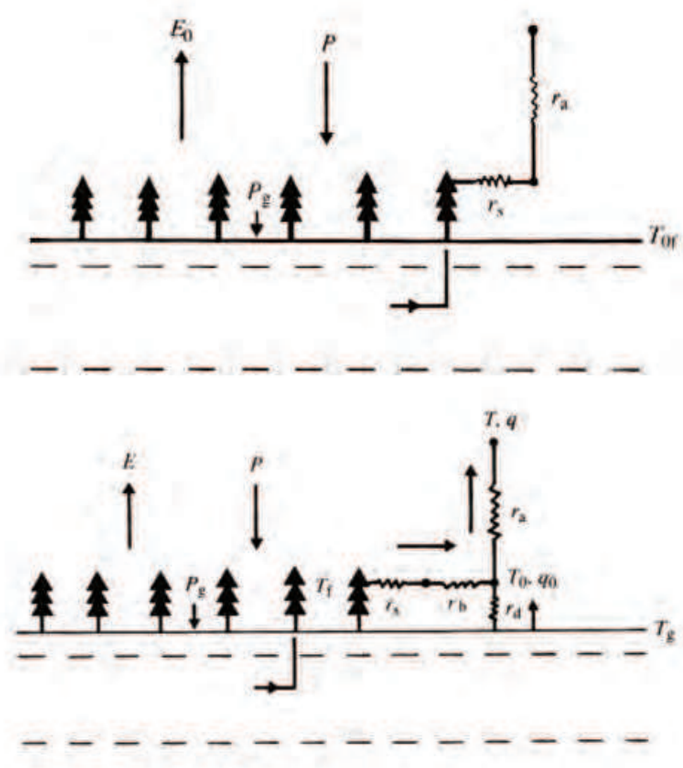

Fig. 5. **Above**: scheme representing a single-layer vegetation model. Linked both with atmosphere (with resistance r_a) and with the deep soil (through evapotranspiration with resistance r_s), vegetation and soil surface layer are assumed to have the same temperature T_{0f}. **Below**: scheme representing a multilayer vegetation model. Linked both with atmosphere (with resistances r_b and r_a), and with the deep soil (through evapotranspiration with resistance r_s), as well as with the soil under the vegetation (r_d), vegetation and soil surface layer are assumed to have different temperature T_f and T_g. P_g is the rainfall reaching the soil surface (from Garratt, 1992).

Given the many uncertainties regarding the forcing data and the components involved (soil, atmosphere), and the numerous simplifying hypotheses, the detail requested in a vegetation cover scheme is not yet clear.

A single-layer description of vegetation cover (big-leaf) and a two-level description of soil represent probably the minimum level of detail requested. In general, if the horizontal scale is far larger than the vegetation scale, a single-layer model is sufficient (Garratt, 1992, p. 242), as in the case of the general circulation atmospheric models or of mesoscale hydrologic models for large basins. These models determine evaporation as if the vegetation cover were but a partially humid plane at the atmosphere basis. In an approach of this kind surface resistance, friction length, albedo and vegetation interception must be specified. The surface resistance must include the dependence on solar radiation or on soil moisture, as transpiration decreases when humidity becomes smaller than the withering point (Jarvis & Morrison, 1981). For the

soil, different coefficients depending on moisture are requested, together with a functional relation of evaporation to the soil moisture.

4. Water in soils

Real evaporation is coupled to the infiltration process occurring in the soil, and its physically-based estimate cannot leave the estimation of soil water content consideration.
The most simple schemes to account water in soils used in LSMs single-layer and two-layer methods. The most general approach, which allows water transport for unsaturated stratified soil, is based on the integration of Richards (1931) equation, under different degrees of approximations.

4.1 Single layer or bucket method

In this method the whole soil layer is considered as a bucket and real evaporation E_0 is a fraction x of potential evaporation E_p, with x proportional to the saturation of the whole soil.

$$E_0 = xE_p \tag{46}$$

with x expressed by Eq. (44). The main problem of this method is that evaporation does not respond to short precipitation, leading to surface saturation but not to a saturation of the whole soil layer (Manabe, 1969).

4.2 Two-layer or force restore method

This method is analogous to the one developed to calculate the soil heat flux, but it requires calibration parameters which are unlikely to be known. With this method it is possible to consider the water quantity used by plants for transpiration, considering a water extraction by roots in the deepest soil layer (Deardorff, 1978).

4.3 Multilayer methods and Richards equation

Richards (1931) equation and Darcy-Buckingham law govern the unsaturated water transport in isobar and isothermal conditions:

$$\vec{q} = -K\nabla\ (z + \psi) \tag{47}$$

$$\frac{\partial \psi}{\partial \eta}\ \nabla \cdot (K\nabla\psi) - \frac{\partial K}{\partial z} = \frac{\partial \psi}{\partial t} \tag{48}$$

where $\vec{q} = (q_x, q_y, q_z)$ is the specific discharge, K is the hydraulic conductivity tensor, z is the upward vertical coordinate and ψ is the suction potential or matrix potential.
The determination of the suction potential allows also a more correct schematization of the plant transpiration and it lets us describe properly flow phenomena from the water table to the surface, necessary to the maintenance of evaporation from the soils.
Richards equation is, rightfully, an energy balance equation, even if this is not evident in the modes from which it has been derived. Then the solutions of the equation (48) must be searched by assigning the water retention curve which relates ψ with the soil water content η and an explicit relation of the hydraulic conductivity as a function of ψ (or η). Both relationships depend on the type of terrain and are variable in every point. K augments with η, until it reaches the maximum value K_s which is reached at saturation.

Although the integration of the Richards equation is the only physically based approach, it requires remarkable computational effort because of the non linearity of the water retention curve. It is difficult to find a representative water retention curve because of the high degree of spatial variability in soil properties (Cordano & Rigon, 2008).

4.4 Spatial variability in soil moisture and evapotranspiration

Topography controls the catchment-scale soil moisture distribution (Beven & Freer, 2001) and therefore water availability for ET. Two methods most frequently used to incorporate sub-grid variability in soil moisture and runoff production SVATs models are the variable infiltration capacity approach (Wood, 1991) and the topographic index approach (Beven & Kirkby, 1979). They represent computationally efficient ways to represent hydrologic processes within the context of regional and global modeling. A review and a comparison of the two methods can be found in Warrach et al. (2002).

More detailed approaches need to track surface or subsurface flow within a catchment explicitly. Such approaches, which require to couple the ET model with a distributed hydrological model, are particularly useful in mountain regions, as presented in the next section.

5. Evapotranspiration in Alpine Regions

In alpine areas, evapotranspiration (ET) spatial distribution is controlled by the complex interplay of topography, incoming radiation and atmospheric processes, as well as soil moisture distribution, different land covers and vegetation types.

1. Elevation, slope and aspect exert a direct control on the incoming solar radiation (Dubayah et al., 1990). Moreover, elevation and the atmospheric boundary layer of the valley affect the air temperature, moisture and wind distribution (e.g., Bertoldi et al., 2008; Chow et al., 2006; Garen & Marks, 2005).
2. Vegetation is organized along altitudinal gradients, and canopy structural properties influence turbulent heat transfer processes, radiation divergence (Wohlfahrt et al., 2003), surface temperature (Bertoldi et al., 2010), therefore transpiration, and, consequently, ET.
3. Soil moisture influences sensible and latent heat partitioning, therefore ET. Topography controls the catchment-scale soil moisture distribution (Beven & Kirkby, 1979) in combination with soil properties (Romano & Palladino, 2002), soil thickness (Heimsath et al., 1997) and vegetation (Brooks & Vivoni, 2008a).

Spatially distributed hydrological and land surface models (e.g., Ivanov et al., 2004; Kunstmann & Stadler, 2005; Wigmosta et al., 1994) are able to describe land surface interactions in complex terrain, both in the temporal and spatial domains. In the next section we show an example of the simulation of the ET spatial distribution in an Alpine catchment simulated with the hydrological model GEOtop (Endrizzi & Marsh, 2010; Rigon et al., 2006).

6. Evapotranspiration in the GEOtop model

The GEOtop model describes the energy and mass exchanges between soil, vegetation and atmosphere. It takes account of land cover, soil moisture and the implications of topography on solar radiation. The model is open-source, and the code can be freely obtained from

the web site: http://www.geotop.org/. There, we provide a brief description of the 0.875 version of the model (Bertoldi et al., 2005), used in this example. For details of the most recent numerical implementation, see Endrizzi & Marsh (2010).
The model has been proved to simulate realistic values for the spatial and temporal dynamics of soil moisture, evapotranspiration, snow cover (Zanotti et al., 2004) and runoff production, depending on soil properties, land cover, land use intensity and catchment morphology (Bertoldi et al., 2010; 2006).
The model is able to simulate the following processes: (i) coupled soil vertical water and energy budgets, through the resolution of the heat and Richard's equations, with temperature and water pressure as prognostic variables (ii) surface energy balance in complex topography, including shadows, shortwave and longwave radiation, turbulent fluxes of sensible and latent heat, as well as considering the effects of vegetation as a boundary condition of the heat equation (iii) ponding, infiltration, exfiltration, root water extraction as a boundary condition of Richard's equation (iv) subsurface lateral flow, solved explicitly and considered as a source/sink term of the vertical Richard's equation (v) surface runoff by kinematic wave, and (vi) multi-layer glacier and snow cover, with a solution of snow water and energy balance fully integrated with soil.
The incoming direct shortwave radiation is computed for each grid cell according to the local solar incidence angle, including shadowing (Iqbal, 1983). It is also split into a direct and diffuse component according to atmospheric and cloud transmissivity (Erbs et al., 1982). The diffuse incoming shortwave and longwave radiation is adjusted according to the theory described in Par. 2.1. The soil column is discretized in several layers of different thicknesses. The heat and Richards' equations are written respectively as:

$$C_t(P)\frac{\partial T}{\partial t} - \frac{\partial}{\partial z}\left[K_t(P)\frac{\partial T}{\partial z}\right] = 0 \tag{49}$$

$$C_h(P)\frac{\partial P}{\partial t} - \frac{\partial}{\partial z}\left[K_h(P)\left(\frac{\partial P}{\partial z} + 1\right)\right] - q_s = 0 \tag{50}$$

Where T is soil temperature, P the water pressure, C_t the thermal capacity, K_t the thermal conductivity, C_h the specific volumetric storativity, K_h the hydraulic conductivity, and q_s the source term associated with lateral flow. The variables C_t, K_t, C_h, and K_h depend on water content, and, in turn, on water pressure, and are therefore a source of non-linearity. At the bottom of the soil column a boundary condition of zero fluxes has been imposed.
The boundary conditions at the surface are consistent with the infiltration and surface energy balance, and are given in terms of surface fluxes of water (Q_h) and heat (Q_t) at the surface, namely:

$$Q_h = min\left[p_{net}, K_{h1}\frac{(h - P_1}{dz/2} + K_{h1}\right] - E(T_1, P_1) \tag{51}$$

$$Q_t = SW_{in} - SW_{out} + LW_{in} - LW_{out}(T_1) - H(T_1) - LE(T_1) \tag{52}$$

Where p_{net} is the net precipitation, K_{h1} and P_1 are the hydraulic conductivity and water pressure of the first layer, h is the pressure of ponding water, dz the thickness of the first layer, T_1 the temperature of the first layer. E is evapotranspiration (as water flux), SW_{in} and SW_{out} are the incoming and outgoing shortwave radiation, LW_{in} and LW_{out} the incoming

and outgoing longwave radiation, H the sensible heat flux and LE the latent heat flux. H and LE are calculated taking into consideration the effects of atmospheric stability (Monin & Obukhov, 1954).
E is partitioned by evaporation or sublimation from the soil or snow surface E_G, transpiration from the vegetation E_{TC}, evaporation of the precipitation intercepted by the vegetation E_{VC}. Every cell has a fraction covered by vegetation and a fraction covered by bare soil. In the 0.875 version of the model, a one-level model of vegetation is employed, as in Garratt (1992) and in Mengelkamp et al. (1999): only one temperature is assumed to be representative of both soil and vegetation. In the most recent version, a two-layer canopy model has been introduced.
Bare soil evaporation E_g is related to the water content of the first layer through the soil resistance analogy (Bonan, 1996):

$$E_G = (1 - cop)\ E_P\ \frac{r_a}{r_a + r_s} \tag{53}$$

where cop is fraction of soil covered by the vegetation EP is the potential ET calculated with equation 34 and r_a the aerodynamic resistance:

$$r_a = 1/\ (\rho\ C_E\ \hat{u}) \tag{54}$$

The soil resistance r_s is function of the water content of the first layer.

$$r_s = r_a\ \frac{1.0 - (\eta_1 - \eta_r)/(\eta_s - \eta_r)}{(\eta_1 - \eta_r)/(\eta_s - \eta_r)} \tag{55}$$

where η_1 is the water content of the first soil layer close the surface, η_r is the residual water content (defined following Van Genuchten, 1980) and η_s is the saturated water content, both in the first soil layer.
The evaporation from wet vegetation is calculated following Deardorff (1978):

$$E_{VC} = cop\ E_P\ \delta_W \tag{56}$$

where δ_W is the wet vegetation fraction.
The transpiration from dry vegetation is calculated as:

$$E_{TC} = cop\ E_P(1 - \delta_W) \sum_i^n \frac{f_{root}^i\ r_a}{r_a + r_c^i} \tag{57}$$

The root fraction f_{root}^i of each soil layer i is calculated decreasing linearly from the surface to a maximum root depth, depending from the cover type. The canopy resistance r_c depends on solar radiation, vapor pressure deficit, temperature as in Best (1998) and on water content in the root zone as in Wigmosta et al. (1994).

6.1 The energy balance at small basin scale: application to the Serraia Lake.

An application of the model to a small basin is shown here, in order to bring out the problems arising when passing from local one-dimensional scale to basin-scale. The Serraia Lake basin is a mountain basin of 9 km^2, with an elevation ranging from 900 to 1900 m, located in Trentino, Italy. Within the basin there is a lake of about 0.5 km^2. During the year 2000 a study to calculate the yearly water balance was performed (Bertola & al., 2002).

The model was forced with meteorological measurement of a station located in the lower part of the basin at about 1000 m, and the stream-flow was calibrated for the sub-catchment of Foss Grand, of about 4 km^2. Then the model was applied to the whole basin. Further details on the calibration can be found in Salvaterra (2001). Meteorological data are assumed to be constant across the basin, except for temperature, which varies linearly with elevation (0.6 ^oC / 100 m) and solar radiation, which slightly increases with elevation and is affected by shadow and aspect.

With the GEO_{TOP} model it is possible to simulate the water and energy balance, aggregated for the whole basin (see figure 6 and 7) and its distribution across the basin. Figure 7 shows the map of the seasonal latent heat flux (ET) in the basin. During winter and fall ET is low (less than 40 W/m^2), with the lowest values in drier convex areas. During summer and spring ET increases (up to 120 W/m^2), with highest values in the bottom of the main valley (where indeed there are a lake and a wetland) and lowest values in north-facing, high-elevation areas.

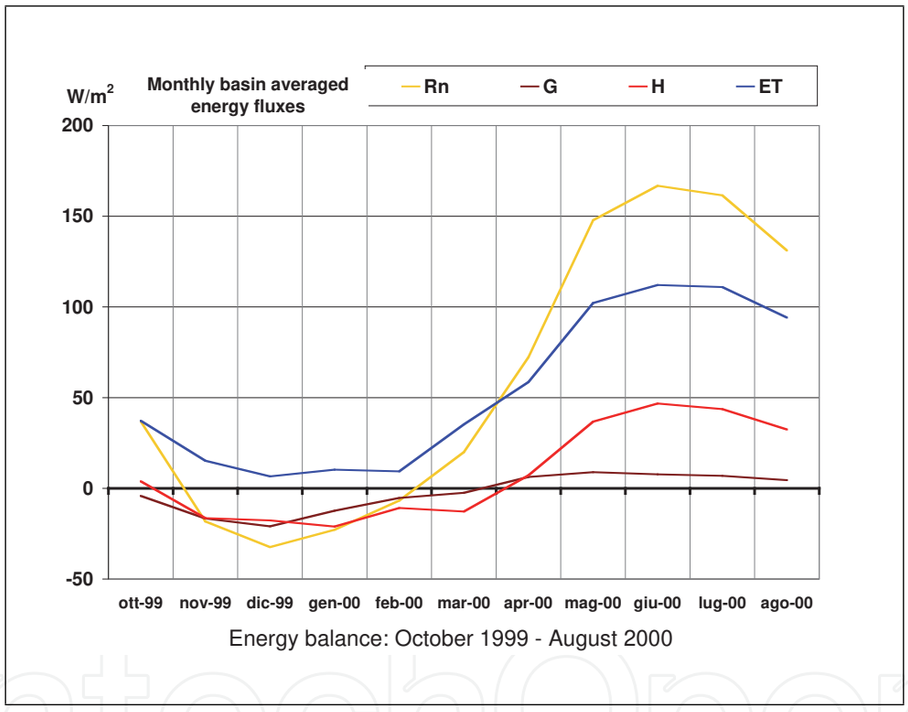

Fig. 6. Monthly energy balance for the Serraia basin (TN, Italy).

The main factors controlling the ET pattern in a mountain environment (see Figure 8) are also: elevation, which controls temperature, aspect, which influences radiation, soil thickness, which determines storage capacity, topographic convergence, which controls the moisture availability. In particular, aspect has a primary effect on net radiation and a secondary effect more on sensible rather than on latent heat flux, as in Figure 9, where south aspect locations have larger R_n and H, but similar behavior for the other energy budget components). Water content changes essentially the rate between latent and heat flux, as in Figure 10 where wet locations have larger ET and lower H.

Therefore, the surface fluxes distribution seems to agree with experience and current hydrology theory, but the high degree of variability poses some relevant issues because the hypothesis of homogenous turbulence at the basis of the fluxes calculation is no more valid

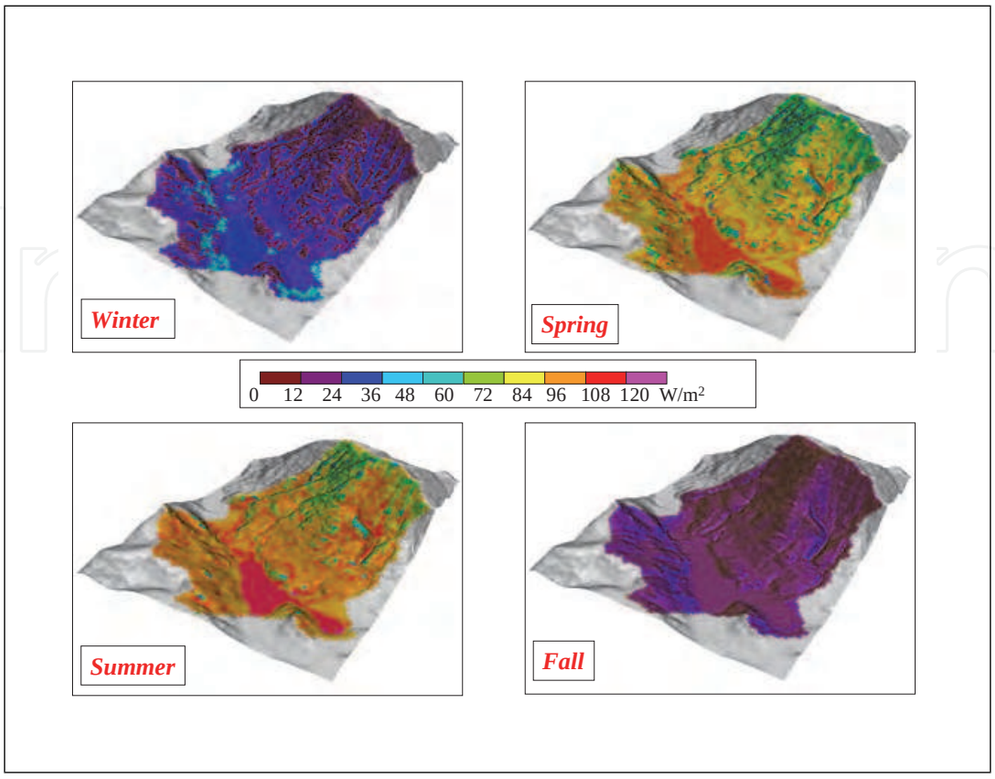

Fig. 7. Seasonal latent heat maps ET $[W/m^2]$ for the Serraia basin (TN, Italy).

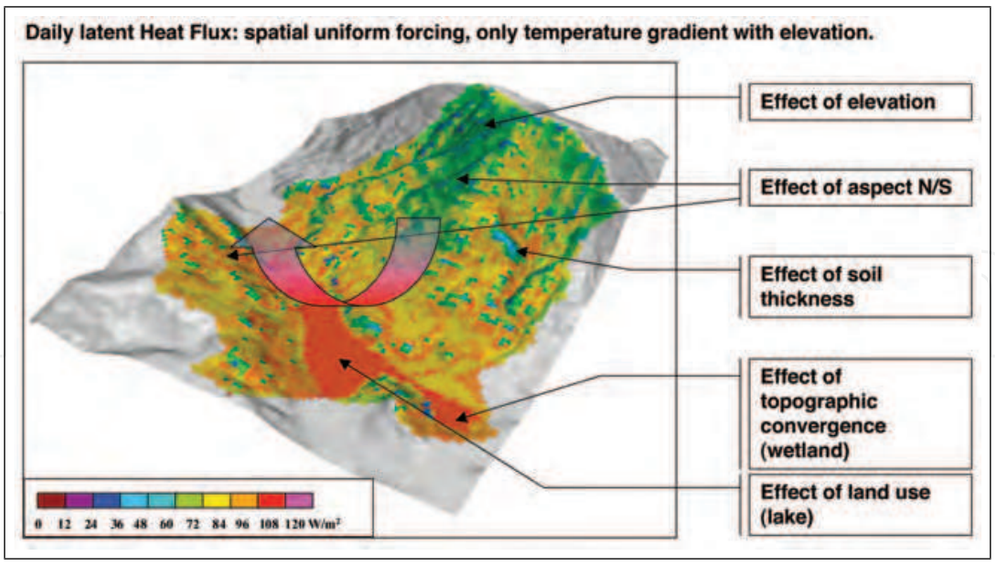

Fig. 8. Example of evapotranspiration ET for the Serraia basin, Italy. Notice the elevation effect (areas more elevated have less evaporation); the aspect effect (more evaporation in southern slopes, left part of the image); the topographic convergence effect on water availability (at the bottom of the valley).

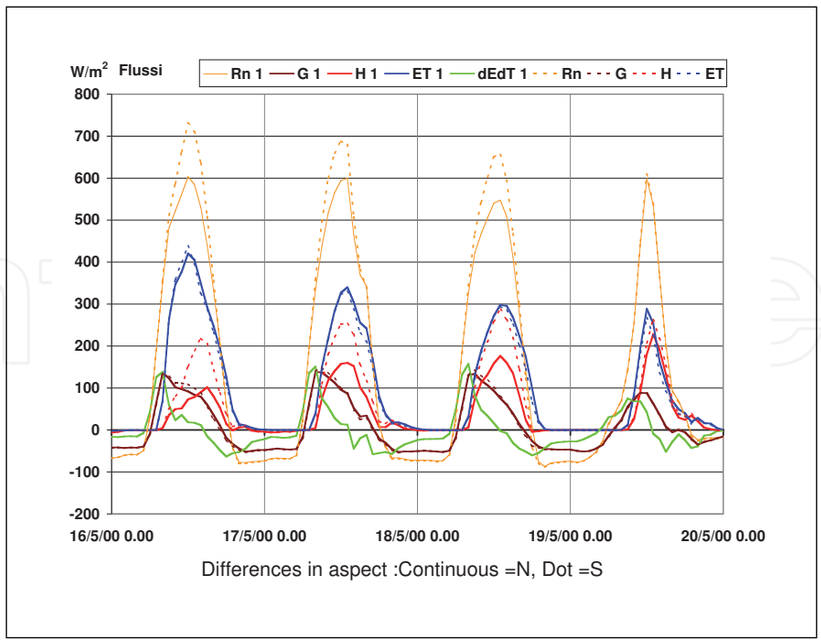

Fig. 9. Difference in energy balance between locations with the same properties but different aspect. Dotted lines are for a south aspect location, while continuos lines are for a north aspect location. It can be noticed how south aspect locations have larger R_n and H, but similar behavior for the other fluxes.

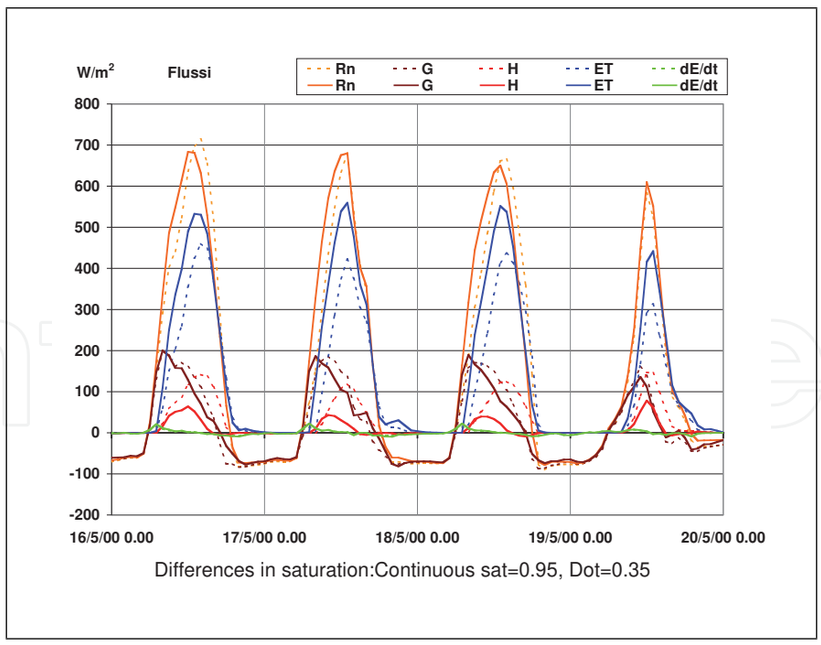

Fig. 10. Difference in energy balance between locations with the same properties but different soil saturation. Dotted lines are for a dry location, while continuos lines are for wet location. It can be noticed how wet locations have larger ET and lower H, but similar behavior for the other fluxes. The time lag in R_n is due to differences in aspect.

(Albertson & Parlange, 1999). Moreover, horizontal differences in surface fluxes can start local air circulations, which can affect temperature and wind surface values with a feedback effect. How much such processes may affect the energy and water balance of the whole basin is easy to quantify, but GEO_{TOP} can be a powerful tool to explore these issues.

7. Conclusion

This chapter illustrates the components of the energy budget needed to model evapotranspiration (ET) and provides an extended review of the fundamental equations and parametrizations available in the hydrological and land surface models literature. In alpine areas, ET spatial distribution is controlled by the complex interplay of topography, incoming radiation and atmospheric processes, as well as soil moisture distribution, different land covers and vegetation types. An application of the distributed hydrological model GEOtop to a small basin is shown here, in order to bring out the problems arising when passing from local one-dimensional scale to basin-scale ET models.

8. References

Albertson, J., Kustas, W. P. & Scanlon, T. M. (2001). Large-eddy simulation over heterogeneous terrain with remotely sensed land surface conditions, *Water Resour. Res.* 37: 1939–1953.

Albertson, J. & Parlange, M. B. (1999). Natural integration of scalar fluxes from complex terrain, *Adv. Water Resour.* 23: 239–252.

Bartelt, P. & Lehning, M. (2002). A physical snowpack model for the swiss avalanche warning: Part i: numerical model, *Cold Regions Science and Technology* 35(3): 123–145.

Bertola, P. & al. (2002). "studio integrato dell'eutrofizzazione del lago della serraia", *Atti del XXVIII Convegno di Idraulica e Costruzioni Idrauliche* 3: 403–413.

Bertoldi, G., Kustas, W. P. & Albertson, J. D. (2008). Estimating spatial variability in atmospheric properties over remotely sensed land-surface conditions, *J. Appl. Met. and Clim.* 47(doi: 10.1175/2007JAMC1828.1): 2147–2165.

Bertoldi, G., Notarnicola, C., Leitinger, G., Endrizzi, S., ad S. Della Chiesa, M. Z. & Tappeiner, U. (2010). Topographical and ecohydrological controls on land surface temperature in an alpine catchment, *Ecohydrology* 3(doi:10.1002/eco.129): 189 – 204.

Bertoldi, G., Rigon, R. & Over, T. (2006). Impact of watershed geomorphic characteristics on the energy and water budgets., *Journal of Hydrometeorology,* 7: 389–403.

Bertoldi, G., Tamanini, D., Endrizzi, S., Zanotti, F. & Rigon, R. (2005). GEOtop 0.875: the programmer's manual, *Technical Report DICA-05-002*, University of Trento E-Prints. In preparation.

Best, M. J. (1998). A model to predict surface temperatures, *Bound. Layer Meteorol.* 88(2): 279–306.

Beven, K. J. & Freer, J. (2001). A dynamic TOPMODEL, *Hydrol. Proc.* 15: 1993–2011.

Beven, K. J. & Kirkby, M. J. (1979). A physically-based variable contributing area model of basin hydrology, *Hydrol. Sci. Bull.* 24(1): 43–49.

Bonan, G. (1996). A land surface model for ecological, hydrological, and atmospheric studies: technical description and user's guide., *Technical Note NCAR/TN-417+STR*, NCAR, Boulder, CO.

Brooks, P. D. & Vivoni, E. R. (2008a). Mountain ecohydrology: quantifying the role of vegetation in the water balance of montane catchments, *Ecohydrol.* 1(DOI: 10.1002/eco.27): 187 – 192.

Brooks, P. & Vivoni, E. R. (2008b). Mountain ecohydrology: quantifying the role of vegetation in the water balance of montane catchments., *Ecohydrology* 1: 187–192.

Brutsaert, W. (1975). On a derivable formula for long-wave radiation from clear skies, *Water Resour. Res.* 11(5): 742–744.

Brutsaert, W. (1982). *Evaporation into the Atmosphere: Theory, Hystory and Applications*, Kluver Academic Publisher.

Businger, J. A., Wyngaard, J. C., Izumi, Y. & Bradley, E. F. (1971). Flux profile relationships in the atmospheric surface layer, *J. Atmospheric Sciences* 28: 181–189.

Chow, F. K., Weigel, A. P., Street, R. L., Rotach, M. W. & Xue, M. (2006). High-resolution large-eddy simulations of flow in a steep alpine valley. Part I: methodology, verification, and sensitivity experiments, *J. Appl. Met. and Clim.* pp. 63–86.

Clapp, R. B. & Hornberger, G. M. (1978). Empirical equations for some hydraulic properties, *Water Resour. Res.* 14: 601–605.

Cordano, E. & Rigon, R. (2008). A perturbative view on the subsurface water pressure response at hillslope scale, *Water Resour. Res.* 44(W05407): doi:10.1029/2006WR005740.

Daamen, C. C. & Simmonds, L. P. (1997). Soil, water, energy and transpiration, a numerical model of water and energy fluxes in soil profiles and sparse canopies, *Technichal report*, University of Reading.

Dall'Amico, M. (2010). *Coupled water and heat transfer in permafrost modeling*, PhD thesis, Institute of Civil and Environmental Engineering, Universita' degli Studi di Trento, Trento. Available from http://eprints-phd.biblio.unitn.it/335/.

Dall'Amico, M., Endrizzi, S., Gruber, S. & Rigon, R. (2011). A robust and energy-conserving model of freezing variably-saturated soil, *The Cryosphere* 5(2): 469–484.
URL: *http://www.the-cryosphere.net/5/469/2011/*

Deardorff, J. W. (1978). Efficient prediction of ground surface temperature and moisture with inclusion of a layer of vegetation, *J. Geophys. Res.* 83(C4): 1889–1903.

Dickinson, R. E., Heanderson-Sellers, A., Kennedy, P. J. & Wilson, M. (1986). Biosphere Atmosphere Transfer Scheme (BATS) for the NCAR Community Climate Model, *Technical Note NCAR/TN-275+STR*, NCAR.

Dubayah, A., Dozier, J. & Davis, F. W. (1990). Topographic distribution of clear-sky radiation over the Konza Prairie, Kansas, *Water Resour. Res.* 26(4): 679–690.

Endrizzi, S., Bertoldi, G., Neteler, M. & Rigon, R. (2006). Snow cover patterns and evolution at basin scale: GEOtop model simulations and remote sensing observations, *Proceedings of the 63rd Eastern Snow Conference*, Newark, Delaware USA, pp. 195–209.

Endrizzi, S. & Marsh, P. (2010). Observations and modeling of turbulent fluxes during melt at the shrub-tundra transition zone 1: point scale variations, *Hydrology Research* 41(6): 471–490.

Erbs, D. G., Klein, S. A. & Duffie, J. A. (1982). Estimation of the diffuse radiation fraction for hourly, daily and monthly average global radiation., *Sol. Energy* 28(4): 293–304.

Feddes, R., Kowalik, P. & Zaradny, H. (1978). Simulation of field water use and crop yield, *Simulation Monographs*, PUDOC, Wageningen, p. 188pp.

Garen, D. C. & Marks, D. (2005). Spatially distributed energy balance snowmelt modelling in a mountainous river basin: estimation of meteorological inputs and verification of model results, *J. Hydrol.* 315: 126–153.

Garratt, J. R. (1992). *The Atmospheric Boundary Layer*, Cambridge University Press.

Heimsath, M. A., Dietrich, W. E., Nishiizumi, K. & Finkel, R. (1997). The soil production function and landscape equilibrium, *Nature* 388: 358–361.

Helbig, N., Lowe, H. & Lehning, M. (2009). Radiosityapproachfortheshortwavesurfaceradiationbalanceincon *J.Atmos.Sci.* 66(doi:10.1175/2009JAS2940.1): 2900–2912.

Iqbal, M. (1983). *An Introduction to Solar Radiation*, Academic Press.

Ivanov, V. Y., Vivoni, E. R., Bras, R. L. & Entekhabi, D. (2004). Catchment hydrologic response with a fully distributed triangulated irregular network model, *Water Resour. Res.* 40: doi:10.1029/2004WR003218.

Jarvis, P. & Morrison, J. (1981). The control of transpiration and photosynthesis by the stomata., *in* P. Jarvis & T. Mansfield (eds), *Stomatal Physiology*, Cambridge Univ. Press, UK, pp. 247–279.

Katul, G. G. & Parlange, M. B. (1992). A penman-brutsaert model for wet surface evaporation, *Water Resour. Res.* 28(1): 121–126.

Kondratyev, K. Y. (1969). *Radiation in the atmosphere*, Academic Press, New York.

Kot, S. C. & Song, Y. (1998). An improvement of the Louis scheme for the surface layer in an atmospheric modelling system, *Bound. Layer Meteorol.* 88(2): 239–254.

Kunstmann, H. & Stadler, C. (2005). High resolution distributed atmospheric-hydrological modelling for alpine catchments, *J. Hydrol.* 314: 105–124.

Law, B. E., Cescatti, A. & Baldocchi, D. D. (1999). Leaf area distribution and radiative transfer in open-canopy forests: Implications to mass and energy exchange., *Tree Physiol.* 21: 287–298.

Louis, J. F. (1979). A parametric model of vertical eddy fluxes in the atmosphere, *Bound. Layer Meteorol.* 17: 187–202.

Manabe, S. (1969). Climate and ocean circulation. i. the atmospheric circulation and the hydrology of the earth's surface., *Monthly Weather Review* 97: 739–774.

Mengelkamp, H., Warrach, K. & Raschke, E. (1999). SEWAB - a parametrization of the surface energy and water balance for atmospheric and hydrologic models, *Adv. Water Resour.* 23: 165–175.

Monin, A. S. & Obukhov, A. M. (1954). Basic laws of turbulent mixing in the ground layer of the atmosphere, *Trans. Geophys. Inst. Akad.* 151: 163–187.

Montaldo, N. & Albertson, J. (2001). On the use of the force-restore svat model formulation for stratified soils, *J. Hydromet.* 2(6): 571–578.

Noilhan, J. & Planton, S. (1989). A simple parametriztion of land surface processes for meteorological models, *Mon. Wea. Rev* 117: 536–585.

Paltrige, G. W. & Platt, C. M. R. (1976). *Radiative Processes in Meteorology and Climatology*, Elsevier.

Parlange, M. B., Eichinger, W. E. & Albertson, J. D. (1995). Regional scale evaporation and the atmospheric boundary layer, *Reviews of Geophysic* 33(1): 99–124.

Philip, J. R. & Vries, D. A. D. (1957). Moisture movement in porous materials under temperature gradients, *Trans. Am. Geophys. Union* 38(2): 222–232.

Prata, A. J. (1996). A new long-wave formula for estimating downward clear-sky radiation at the surface., *Quarterly Journal of the Royal Meteorological Society* 122(doi: 10.1002/qj.49712253306): 1127–1151.

Richards, L. A. (1931). Capillary conduction of liquids in porous mediums, *Physics* 1: 318–333.

Rigon, R., Bertoldi, G. & Over, T. M. (2006). GEOtop: a distributed hydrological model with coupled water and energy budgets, *Journal of Hydrometeorology* 7: 371–388.

Romano, N. & Palladino, M. (2002). Prediction of soil water retention using soil physical data and terrain attributes, *J. Hydrol.* 265: 56–75.

Salvaterra, M. (2001). *Applicazione di un modello di bilancio idrologico al bacino del Lago di Serraia (TN)*, Tesi di diploma, Corso di diploma in Ingegneria per l'Ambiente e le Risorse.

Saravanapavan, T. & Salvucci, G. D. (2000). Analysis of rate-limiting processes in soil evaporation with implications for soil resistance models, *Adv. Water Resour.* 23: 493–502.

Scanlon, T. M. & Albertson, J. D. (2003). Water availability and the spatial complexity of co2, water, and energy fluxes over a heterogeneous sparse canopy, *J. Hydromet.* 4(5): 798–809.

Stull, R. B. (1988). *An Introduction to Boundary Layer Meteorology*, Kluwer Academic Publisher.

Van Genuchten, M. T. (1980). A closed-form equation for predicting the hydraulic conductivity of unsaturated soils., *Soil Sci. Soc. Am. J.* 44: 892–898.

Warrach, K., Stieglitz, M., Mengelkamp, H. & Raschke, E. (2002). Advantages of a topographically controlled runoff simulation in a SVAT model, *J. Hydromet.* 3: 131–148.

Wigmosta, M. S., Vail, L. & Lettenmaier, D. (1994). A Distributed Hydrology-Vegetation Model for complex terrain, *Water Resour. Res.* 30(6): 1665–1679.

Wohlfahrt, G., Bahn, M., Newesely, C. H., Sapinsky, S., Tappeiner, U. & Cernusca, A. (2003). Canopy structure versus physiology effects on net photosynthesis of mountain grasslands differing in land use., *Ecological modelling.* 170: 407–426.

Wood, E. F. (1991). Land-surface-atmosphere interactions for climate modelling. observations, models and analysis, *Surv. in Geophys.* 12: 1–3.

Zanotti, F., Endrizzi, S., Bertoldi, G. & Rigon, R. (2004). The geotop snow module, *Hydrol. Proc.* 18: 3667–3679. DOI:10.1002/hyp.5794.

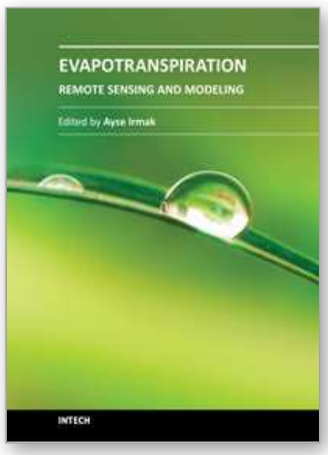

Evapotranspiration - Remote Sensing and Modeling

Edited by Dr. Ayse Irmak

ISBN 978-953-307-808-3
Hard cover, 514 pages
Publisher InTech
Published online 18, January, 2012
Published in print edition January, 2012

This edition of Evapotranspiration - Remote Sensing and Modeling contains 23 chapters related to the modeling and simulation of evapotranspiration (ET) and remote sensing-based energy balance determination of ET. These areas are at the forefront of technologies that quantify the highly spatial ET from the Earth's surface. The topics describe mechanics of ET simulation from partially vegetated surfaces and stomatal conductance behavior of natural and agricultural ecosystems. Estimation methods that use weather based methods, soil water balance, the Complementary Relationship, the Hargreaves and other temperature-radiation based methods, and Fuzzy-Probabilistic calculations are described. A critical review describes methods used in hydrological models. Applications describe ET patterns in alpine catchments, under water shortage, for irrigated systems, under climate change, and for grasslands and pastures. Remote sensing based approaches include Landsat and MODIS satellite-based energy balance, and the common process models SEBAL, METRIC and S-SEBS. Recommended guidelines for applying operational satellite-based energy balance models and for overcoming common challenges are made.

InTech Europe
University Campus STeP Ri
Slavka Krautzeka 83/A
51000 Rijeka, Croatia
Phone: +385 (51) 770 447
Fax: +385 (51) 686 166
www.intechopen.com

InTech China
Unit 405, Office Block, Hotel Equatorial Shanghai
No.65, Yan An Road (West), Shanghai, 200040, China
中国上海市延安西路65号上海国际贵都大饭店办公楼405单元
Phone: +86-21-62489820
Fax: +86-21-62489821

IntechOpen